Radiology

Optoacoustic Imaging of Human Vasculature: Feasibility by Using a Handheld Probe[1]

Adrian Taruttis, DEng
Arwin C. Timmermans
Philip C. Wouters, MD
Marcin Kacprowicz, MS
Gooitzen M. van Dam, MD, PhD
Vasilis Ntziachristos, PhD

Purpose: To investigate whether multispectral optoacoustic tomography (MSOT) developed for deep-tissue imaging in humans could enable the clinical assessment of major blood vessels and microvasculature.

Materials and Methods: The study was approved by the Institutional Review Board of the University Medical Center Groningen (CCMO-NL-43587) and registered in the Dutch National Trial Registry (NTR4125). The authors designed a real-time handheld optoacoustic scanner for human use, based on a concave 8-MHz transducer array, attaining 135° angular coverage. They applied a single-pulse-frame (SPF) sequence, which enabled motion insensitive optoacoustic imaging during handheld operation. SPF optoacoustic imaging was applied to imaging arteries and microvascular landmarks in the lower extremities of 10 healthy volunteers. The diameters selected microvessels were determined by measuring the full width at half maximum through the vessels in the MSOT images. Duplex ultrasonography was performed on the same landmarks in seven of the 10 volunteers for subjective comparison to the corresponding optoacoustic images.

Results: Optoacoustic imaging resolved blood vessels as small as 100 μm in diameter and within 1 cm depth. Additionally, MSOT provided images reflecting hemoglobin oxygen saturation in blood vessels, clearly identifying arteries and veins, and was able to identify pulsation in arteries during imaging. Larger blood vessels, specifically the tibialis posterior and the dorsalis pedis arteries, were also visualized with MSOT.

Conclusion: Handheld MSOT was found to be capable of clinical vascular imaging, providing visualization of major blood vessels and microvasculature and providing images of hemoglobin oxygen saturation and pulsation.

[1] From the Department of Surgery, University Medical Center Groningen, University of Groningen, Groningen, the Netherlands (A.T., A.C.T., P.C.W., G.M.v.D.); iThera Medical GmbH, Munich, Germany (M.K.); Institute for Biological and Medical Imaging, Helmholtz Zentrum München, Neuherberg, Germany (V.N.); and Department of Biological Imaging, Technische Universität München, Ismaninger Str 22, Munich, Germany (V.N.). Received October 1, 2015; revision requested November 2; final revision received February 3, 2016; accepted February 18; final version accepted June 2. **Address correspondence to** V.N. (e-mail: *v.ntziachristos@tum.de*).

V.N. supported by European Research Council (Advanced Grant 233161 Next Generation in-vivo im). Supported by Deutsche Forschungsgemeinschaft (Forschungsstipendium). A.T. supported by a Research Fellowship from the German Research Foundation (DFG TA 953/1-1).

Vascular diseases of the extremities, including peripheral arterial disease, diabetic foot, and (autoimmune) vasculitis, lead to morbidity as a result of limited blood supply to the peripheral tissue. In current clinical practice, the assessment of peripheral tissue blood supply is performed indirectly by characterizing the morphology of large arteries and blood flow within them by using duplex ultrasonography (US). Alternative methods include assessment of the ankle-brachial blood pressure index and digital subtraction angiography, magnetic resonance angiography, or computed tomographic angiography (1,2). Transcutaneous oxygen tension ($TcPO_2$) measurements can be used to obtain an estimate for oxygen delivery at a point on the skin, but the method does not allow visualization of blood vessels.

Duplex US is the most commonly applied method in clinical vascular assessment. The modality is targeted at larger scale blood vessels. Doppler US can depict flow and therefore can better reveal blood vessels and characterize blood flow within them. However, Doppler flow and power Doppler signals display an inherent lack of sensitivity that results in a loss of image fidelity in small blood vessels and an inability to visualize microvasculature.

The visualization of small-diameter blood vessels could fill an important gap in current vascular imaging practice. The performance of amputations after revascularization in patients with limb ischemia indicates the need for improved methods to predict outcomes in patients who are candidates for revascularization (3,4). Imaging of large blood vessels as well as vessels with microvascular dimensions could help to better characterize the distribution of microcirculation in patients with critical limb ischemia or diffuse multisegment disease (2), potentially providing improved prediction of the success of revascularization. Furthermore, the imaging of hemoglobin and its oxygenation status could provide a more complete characterization of arterial lesions, for example, characterization of the vasa vasorum or of thrombosis could provide new information on the stability of atherosclerotic plaques (5).

The contrast in optoacoustic vascular imaging does not rely on blood flow; instead, it is generated by the strong optical absorption of hemoglobin. Therefore, optoacoustic imaging of vasculature can be achieved because hemoglobin is concentrated in blood vessels and accurately delineates them. In particular, multispectral optoacoustic tomography (MSOT) sequentially illuminates tissue at multiple wavelengths and then applies spectral unmixing algorithms on the resulting optoacoustic images to resolve multiple individual absorbers (eg, oxyhemoglobin, deoxyhemoglobin, melanin, optical contrast agents) based on their distinct absorption spectrum (6). MSOT can therefore also be used to visualize oxygenation or blood saturation by independently resolving oxygenated and deoxygenated hemoglobin. Optoacoustic and MSOT methods in various forms have been demonstrated for cancer imaging (7,8), including the visualization of tumor vasculature at large scales in human subjects (9,10) and small scales in animal studies (11,12).

Optoacoustic imaging of vasculature has been previously demonstrated for superficial vessels, typically in the skin (13–15), by using high-frequency US arrays (eg, 25 MHz) or by raster scanning focused illumination, achieving optical diffraction-limited resolution within the first millimeter of tissue (16). However, optoacoustic imaging deeper in tissues has only so far revealed larger scale vessels, such as the carotid arteries (17). Original handheld optoacoustic imaging systems utilized linear-array US transducers common to clinical US imaging devices (18–21). This design uses broadly available linear US arrays and can offer the seamless integration of US and optoacoustic imaging in one hybrid modality. However, optoacoustic image quality substantially improves when using curved (concave) US arrays that cover multiple angles around the region of interest (17). While conventional US imaging transmits and receives ultrasound signals, optoacoustic imaging only relies on receiving omnidirectional ultrasound signals from the entire volume illuminated. Therefore, the detector geometry and the inversion technique used play a more critical role in optoacoustic image formation than in US imaging. In addition, the utilization of concave arrays provides space for illumination of the imaged section, while linear arrays necessitate out-of-plane illumination.

To study MSOT imaging of human vasculature, we developed a curved geometry (135° coverage) portable handheld scanner, optimized to image within 1 cm of tissue depth. The system was based on a new generation of wavelength-tuning optical parametric oscillator technology that can deliver up to 50 different wavelengths per second (22), allowing video-rate multispectral operation. The system therefore

Advances in Knowledge

- Vascular imaging in the extremities by means of bedside handheld multispectral optoacoustic tomography, displaying hemoglobin oxygenation in real time, is feasible.
- The imaging system studied visualized the tibialis posterior artery and dorsalis pedis artery as well as small vessels down to a diameter of approximately 100 μm.

Published online before print
10.1148/radiol.2016152160 **Content codes:** US VA

Radiology 2016; 000:1–8

Abbreviations:
CNR = contrast-to-noise ratio
MSOT = multispectral optoacoustic tomography

Author contributions:
Guarantors of integrity of entire study, A.T., G.M.v.D., V.N.; study concepts/study design or data acquisition or data analysis/interpretation, all authors; manuscript drafting or manuscript revision for important intellectual content, all authors; approval of final version of submitted manuscript, all authors; agrees to ensure any questions related to the work are appropriately resolved, all authors; literature research, A.T., A.C.T., M.K.; clinical studies, A.T., A.C.T., P.C.W., M.K., G.M.v.D.; experimental studies, A.T., A.C.T., P.C.W., M.K.; statistical analysis, A.C.T., M.K.; and manuscript editing, A.T., A.C.T., M.K., G.M.v.D., V.N.

Conflicts of interest are listed at the end of this article.

combines macro- and microscale blood vessel imaging with real-time handheld multispectral operation, acquiring one cross-sectional frame per pulse (< 30 μsec per frame), therefore minimizing motion effects. We investigated the vascular imaging capabilities of the system in human volunteers and compared its performance to that of duplex US. Our purpose was to investigate whether MSOT imaging developed for deep-tissue imaging in humans could enable the clinical assessment of major blood vessels and microvasculature.

Materials and Methods

The MSOT imaging platform utilized in this study was provided on loan by iThera Medical (Munich, Germany) to the University Medical Center Groningen (the Netherlands). V.N. is a shareholder of iThera Medical. In addition, V.N. has a patent US 20140198606 A1/EP2754388A1 issued, a patent WO 2012103903 A1 issued, a patent WO2011098101A1; PCT/EP2010/006937, a patent WO 2011000389 A1 issued, a patent EP2148183 issued, a patent PCT/EP2008/006142 issued, and a patent US 61/066,187; PCT/EP2009/001137 issued, which are directly or indirectly relevant to the work. M.K. is an employee of iThera Medical. In addition, M.K. has a patent US20140221810 A1 pending, a patent EP2742854A1 pending, and a patent CN103860140A issued, which are relevant to the work. A.T. had full control over the inclusion of data or information.

Healthy Volunteers

The study protocol was approved by the Institutional Review Board of the University Medical Center Groningen (CCMO-NL-43587) and registered in the Dutch National Trial Registry (NTR4125). Inclusion criteria were healthy volunteers, at least 18 years of age, written informed consent, and adequate potential for telephone follow-up after the procedure. Exclusion criteria were medical or psychiatric conditions that compromised the volunteers' ability to give informed consent, concurrent uncontrolled medical conditions, any investigational treatment for peripheral vascular disease or lower leg fractures within the past month, pregnancy or breast feeding, clinically significant (ie, active) cardiovascular disease (eg, congestive heart failure, symptomatic coronary artery disease and cardiac dysrhythmia, eg, atrial fibrillation, even if controlled with medication, peripheral vascular disease) or myocardial infarction within the past 12 months, symptoms or history of peripheral neuropathy, (partial) amputation of one of the legs. The healthy volunteers consisted of five men and five women (mean age, 28 years; range, 20–46 years; skin types I-III on the Fitzpatrick scale [23]). Their health status was verified by their medical history and physical examination, including blood pressure measurement, pulse oximetry, and the ankle-brachial index. After MSOT imaging, the subjects were questioned about any unpleasant sensations during or after the procedure, and the lower extremities were examined for any skin changes to check for any unexpected thermal damage from laser exposure. Approximately 2 weeks after imaging, the subjects were contacted again and questioned about possible side-effects. The start date of the study was December 21, 2013; the end date was January 30, 2014.

Single-Pulse-Frame Curved-Array MSOT

A curved-array handheld MSOT head was developed (Fig 1a) for portable use in analogy to diagnostic US imaging. Important characteristics are the geometry of the US transducer array and the interface of the scanner onto tissue in handheld mode (Fig 1b). Optoacoustic signals are detected by using a custom 128-element transducer array with a focal length of 2 cm and a central frequency of 8 MHz (Imasonic SaS, Voray, France). The elements are arranged in one row facing inward on an arc covering 135°. The concave shape allows for better reconstruction of optoacoustic images compared with a linear array (15). In addition, the concave arc allows space for the light pulses to illuminate the skin in the detection plane, therefore reducing out-of-plane artifacts and making better use of the available light energy than in the case of out-of-plan illumination. Light is delivered via an optical fiber-bundle assembly (Light Guide Optics, Rheinbach, Germany) integrated within the imaging probe.

Laser illumination and optoacoustic signal detection are provided by an MSOT system (EIP-100; iThera Medical). The imaging system is capable of displaying and storing 50 frames per second. However, to maximize the permissible laser illumination energy, we used a frame rate of 10 frames per second. Light fluence on the skin was limited to stay below the maximum permissible exposure limits according to the applicable laser safety standard (IEC 60825–1). Pulsed light was delivered by a diode-pumped Nd:YAG laser pumping an optical parametric oscillator for wavelength tuning in the near infrared range (InnoLas Laser, Krailing, Germany). Signals were acquired by a custom 12-bit digitizer with a sampling rate of 40 megasamples per second. The single-pulse-frame sequence recorded one full frame at a single wavelength utilizing only one pulse. Therefore, the data for each frame were recorded within approximately 30 μsec, that is, the time for sound propagation from the tissue imaged to the detector. This approach minimizes motion artifacts on the images and provides fast multispectral acquisition. Optoacoustic images were acquired at four optical wavelengths: 730 nm, 750 nm, 800 nm, and 830 nm, which are suitable for resolving the differences in absorption spectra between oxygenated and deoxygenated hemoglobin. As a result, the frame rate for multispectral images at four wavelengths was 2.5 Hz.

Image Reconstruction and Analysis

Data captured at each wavelength were reconstructed by using a semi-analytical model-based algorithm (24,25), utilizing a parallelized OpenCL (Khronos Group, Beaverton, Ore) image reconstruction algorithm running on a graphics processing unit. Spectral

Figure 1

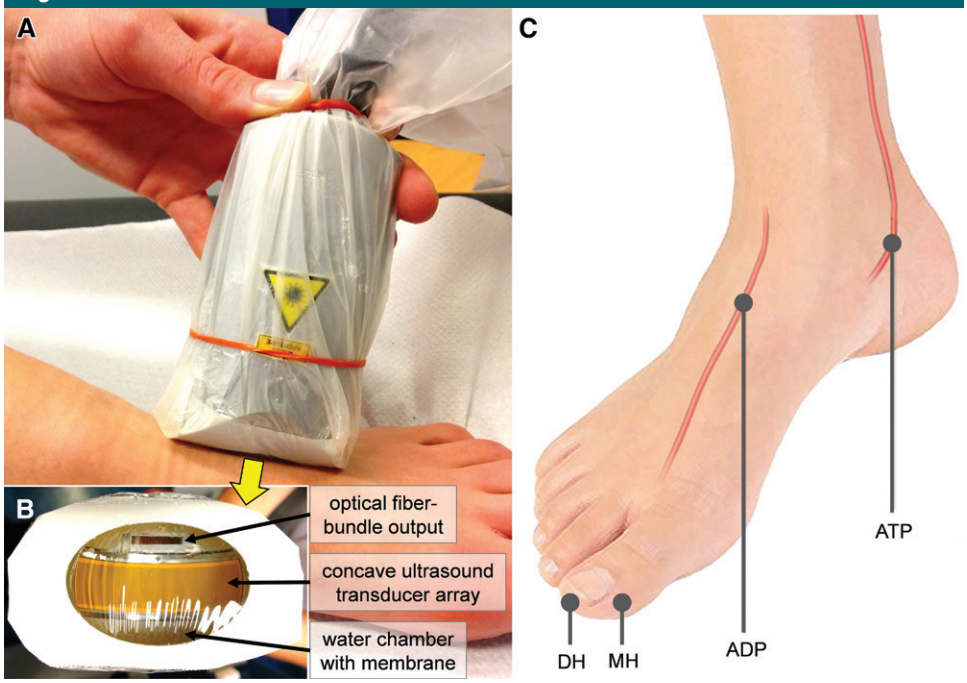

Figure 1: *A,* Handheld optoacoustic imaging probe as utilized to image the dorsalis pedis artery in the foot. *B,* Front view of the handheld optoacoustic imaging probe. The US transducer array has a concave shape with an angular coverage of 135°. It provides space for light from the fiber-bundle to illuminate the skin in the imaging plane. *C,* Vascular imaging landmarks on the foot. *ADP* = dorsalis pedis artery, *ATP* = tibialis posterior artery, *MH* = medial hallux, *DH* = distal hallux.

unmixing was applied by using nonnegative least squares to produce images of oxy- and deoxyhemoglobin (26). To compute hemoglobin oxygen saturation (SO_2), the oxyhemoglobin (HbO_2) and deoxyhemoglobin (Hb) images were placed into the following formula on a per-pixel basis: $SO_2 = HbO_2/(HbO_2 + Hb)$. Contrast-to-noise ratios (CNRs) were computed on the 830-nm images by manually selecting three regions: a 10 × 10-pixel square within the target blood vessel, a 10 × 10-pixel square adjacent to the target blood vessel to represent the background, and a 50 × 50-pixel square outside of the tissue to estimate the image noise. The difference between the means of the target and background pixels divided by the standard deviation of the noise pixels then provides the CNR. The depth of the blood vessels for which the CNR was computed was found by drawing a line on the optoacoustic images from the skin surface to the edge of the blood vessel closest to the skin. To determine the approximate scale of the smallest blood vessels present on the MSOT images, the diameters of the selected blood vessels were extracted from the MSOT images of oxyhemoglobin by drawing a line through the vessel and determining the full width at half maximum of the image pixel values on that line. All analyses were performed by A.T. and checked by A.C.T and P.C.W., without being blinded to any information.

Imaging Landmarks and Protocol

We imaged predefined landmarks in the lower extremities that are relevant to peripheral arterial disease (Fig 1c). Two peripheral arteries and two microvascular landmarks were imaged, that is, the dorsalis pedis and tibialis posterior arteries and medial and distal hallux, respectively. The handheld MSOT probe was positioned on the landmark, and clear US gel (Aquasonic 100; Parker Laboratories, Fairfield, NJ) was applied for acoustic coupling. Real-time imaging allowed for swift localization of the target arteries. Duplex US was performed at a later date (up to 40 days later) on the same landmarks for comparison. At the landmarks for assessing the microvasculature, the duplex US signal intensity was increased until a vascular structure was identifiable or the image consisted of noise.

MSOT imaging was performed by A.T., A.C.T. and P.C.W. US imaging was performed by two practicing vascular technologists with 24 years and 4 years of experience. US imaging was performed in seven of the 10 volunteers; the rest were not available for a second visit. US examinations were performed by using an Acuson S2000 machine (Siemens Healthcare, Erlangen, Germany) with an Acuson 18L6 HD probe (Siemens), which is a linear-array transducer with a 5.5–18-MHz

frequency bandwidth. Tissue harmonic imaging at 12 MHz was active. Color Doppler velocity imaging at 7.5 or 9 MHz was used to visualize blood flow. For imaging the hallux, additional US gel was used so that the focal zone of the probe was correctly positioned with respect to the imaged tissue.

Results

No skin damage, side effects, or any adverse events resulting from the MSOT imaging procedures were observed.

Large Arteries

To investigate the performance of MSOT imaging of large arteries, we imaged the tibialis posterior (ATP) and dorsalis pedis (ADP) arteries (Fig 2). The MSOT images show clearly defined blood vessels carrying oxygenated blood, corresponding to duplex US images. The target blood vessels, once localized by using the handheld MSOT device, were visible with high contrast from the background. In images of the ADP, the mean CNR was 22.4 (minimum, 11; maximum, 50; n = 10). For the ATP, the mean CNR was 14.3 (minimum, 5; maximum, 33; n = 10). The ATP lies deeper beneath the skin surface than the ADP: The mean depth for the ATP was 5.1 mm (minimum, 3.8 mm; maximum, 6.8 mm) compared with 3.1 mm (minimum, 2.2 mm; maximum, 5.5 mm) for the ADP. The deepest structures visible without additional postprocessing during imaging in this study were at a depth of approximately 10 mm beneath the skin.

Small Blood Vessels

To investigate the performance of MSOT in imaging of small blood vessels in peripheral tissue, imaging was performed on the medial and distal hallux (Fig 3). In addition to displaying millimeter-sized blood vessels, MSOT was able to resolve microvasculature carrying oxygenated hemoglobin on the order of less than 100 μm, which was not visible on the corresponding duplex US images. Furthermore, blood vessels

Figure 2

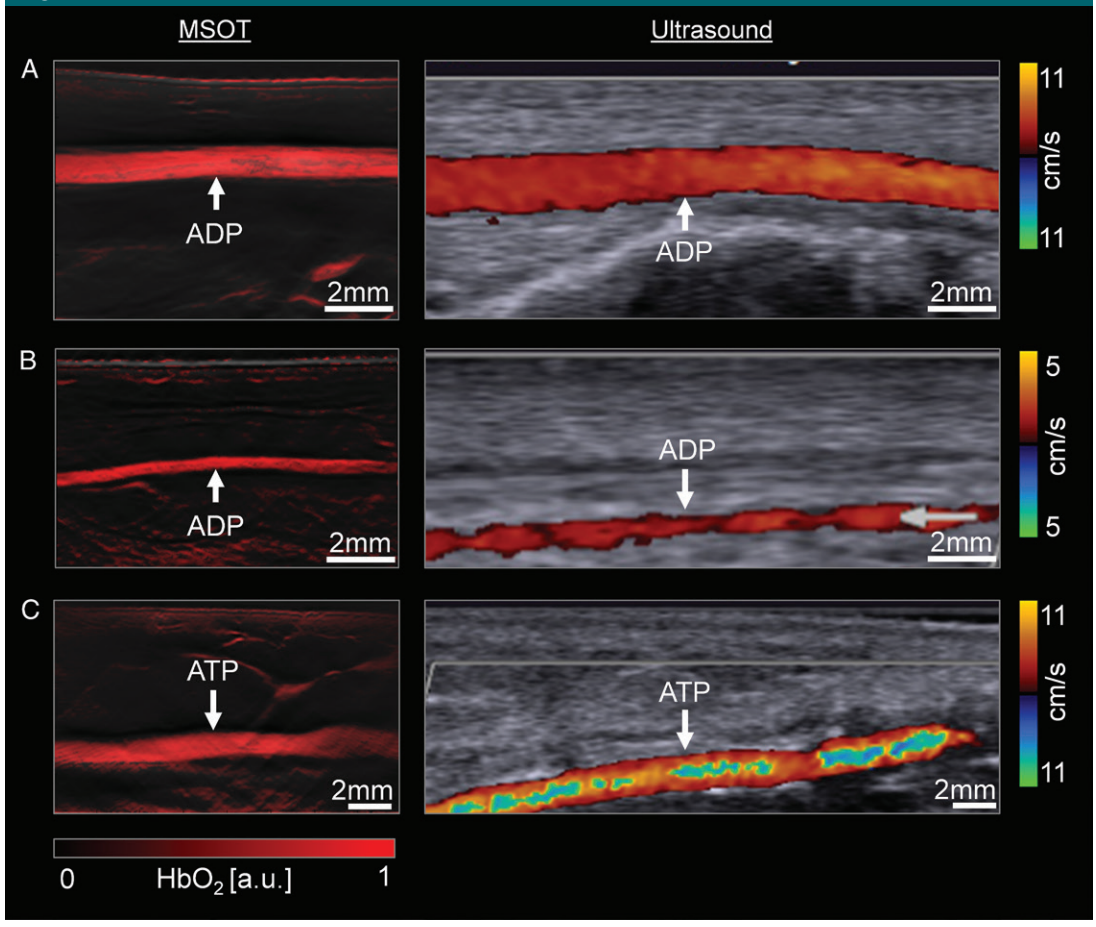

Figure 2: MSOT imaging of arteries. Left column shows MSOT images, where oxyhemoglobin signal is superimposed in red on gray-scale images acquired at 830 nm. Right column shows duplex US images. All images are cropped to a region of interest. The skin is at the top of each panel so that MSOT and US images are approximately aligned. A, Dorsalis pedis artery *(ADP). B,* ADP in a subject where this artery is smaller than usual. *C,* Tibialis posterior artery *(ATP). a.u.* = arbitrary unit.

Figure 3

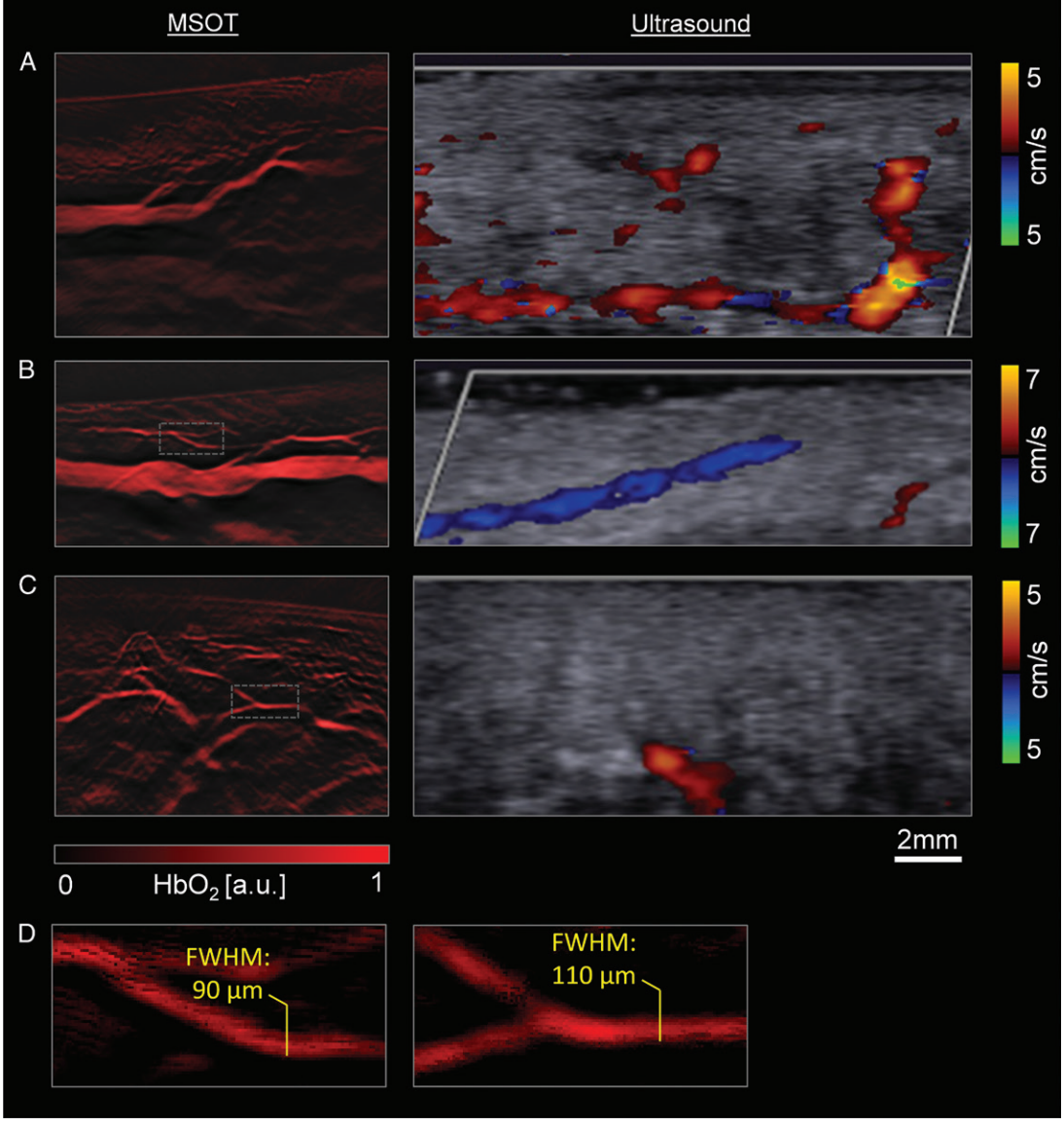

Figure 3: MSOT imaging of small blood vessels. Left column shows MSOT images, where oxyhemoglobin signal is superimposed in red on images acquired at 830 nm. Right column shows duplex US images. All images are cropped to a region of interest. The skin is at the top of each panel so that MSOT and US images are approximately aligned. *A, B,* Medial side of the hallux in two different subjects. *C,* Distal tip of the hallux. MSOT hemoglobin contrast provides more sensitive detection of small blood vessels than does clinical Doppler US. *D,* Zoomed-in MSOT images of the regions indicated by boxes in, *B,* and, *C,* show features belonging to the smallest structures clearly identified as blood vessels. The diameters at the yellow lines are provided as the full width at half maximum *(FWHM). a.u.* = arbitrary unit.

of these and similar dimensions were resolved in all 10 volunteers at depths up to approximately 5 mm.

Hemoglobin Oxygenation and Pulsatility

Distinction between arteries and veins on MSOT images is enabled by the difference in oxygenation between arterial and venous blood, as shown in Figure 4. The separate images of oxygenated and deoxygenated hemoglobin can be displayed either in a dual-color representation of the intensities of each of the signals or as a per-pixel representation of hemoglobin oxygen saturation. Finally, because optoacoustic imaging was performed in real time, where each laser pulse produces an image frame, it is possible to resolve the arterial pulse as seen in Figure 4c.

Figure 4

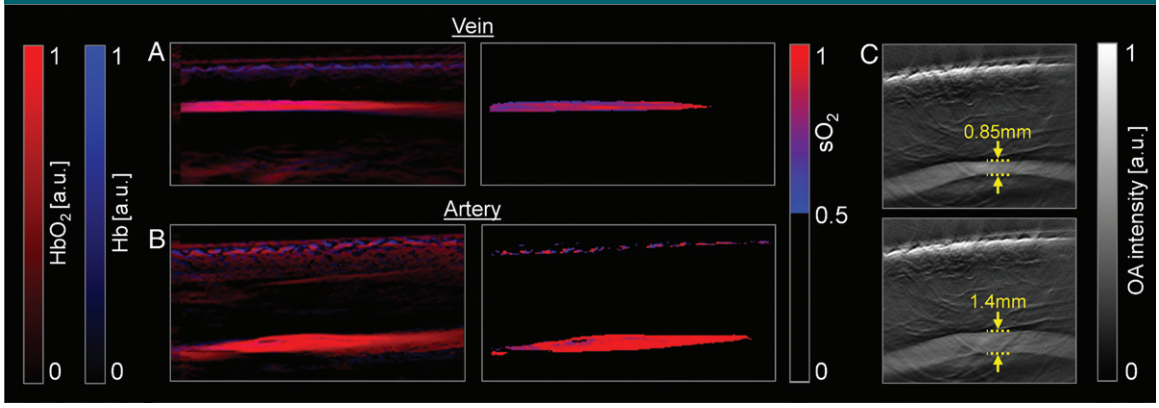

Figure 4: *A, B,* MSOT distinguishes veins from arteries by means of hemoglobin oxygenation. Left: Oxyhemoglobin (HbO_2) and deoxyhemoglobin (Hb) intensities in red and blue, respectively. Right: Hemoglobin oxygen saturation (SO_2). *C,* Consecutive image frames at 830 nm resolve a change in the diameter of an artery (tibialis posterior artery). These two frames are 400 msec apart. *a.u.* = arbitrary unit.

Discussion

A clinical study in healthy volunteers was performed to assess the feasibility of a curved-array handheld MSOT system for vascular imaging of the foot, particularly in comparison with standard duplex US. Our results show that MSOT provides visualization of large blood vessels and can simultaneously resolve smaller vasculature. This imaging performance is based on the high sensitivity of optoacoustic imaging to hemoglobin and broadband nature of the optoacoustic signals. While Doppler US measures flow, MSOT resolves hemoglobin in its oxygenated and deoxygenated states by means of optical absorption. The MSOT system utilized in our study has a handheld implementation similar to diagnostic US and is capable of displaying multispectral images in real time.

The findings herein indicate that MSOT, either as an add-on to US or as a separate device, could become an integral part of clinical vascular workup, providing a more detailed view of small vessels and oxygenated hemoglobin delivery. MSOT vascular imaging could be utilized for disease assessment and therapeutic monitoring, as well as follow-up after vascular interventions such as stent placement, bypass surgery, and rehabilitation programs.

Beyond imaging blood vessels and noninvasive assessment of their oxygenation as shown in our study, MSOT can resolve a number of potential biomarkers of vascular disease. Lipids (27), neovasculature, or thrombi may be visualized. Additionally, a growing toolbox of exogenous agents that absorb light is detectable with MSOT, providing the means for simultaneous molecular, functional, and physiologic imaging (28). The ability to image inflammation, in particular, by using exogenous targeted optoacoustic imaging contrast agents, which has been demonstrated in mouse models (29), could provide improved clinical risk stratification in cardiovascular disease, if the agents gain regulatory approval.

Optoacoustic imaging is highly scalable in terms of spatial resolution. The implementation chosen for this study was able to image blood vessels down to a diameter of approximately 100 μm and produced images showing structures at a penetration depth of approximately 1 cm. By increasing the detector frequency and adjusting its dimensions, a higher resolution would be obtainable at the expense of field of view and tissue penetration depth. For example, optoacoustic imaging at 18-μm transverse resolutions have been demonstrated without using focused light (15), which indicates that the approach could be scaled down if visualization of smaller microvasculature is necessary.

Conversely, by sacrificing spatial resolution, the penetration depth could be increased. Penetration depths of several centimeters have been demonstrated in optoacoustic imaging of blood vessels in whole breasts (30). The selection of an appropriate scale for imaging depends on the diagnostic application. However, optoacoustic imaging is inherently limited in penetration depth by the use of light for excitation. Furthermore, because acoustic detection is applied, some of the typical limitations of US also hold for optoacoustic imaging: Thick bones and pockets of air (eg, in the lungs) will degrade images.

The limitations of this study will need to be addressed in future studies. In particular, the study only included healthy volunteers and therefore could not show which aspects of vascular disease are detectable with MSOT. Additionally, the exact comparison of blood vessels imaged with MSOT and US was hampered by the difficulty in imaging exactly the same tissue slice with both techniques also because the imaging was performed by different people on different days. No reference standard was used for the hemoglobin oxygenation images, therefore preventing assessment of their accuracy. The quantitative accuracy of hemoglobin unmixing is a topic of current research (31,32).

We conclude from our study that handheld MSOT imaging of large blood vessels and microvessels by hemoglobin

contrast in humans is feasible, providing a view of the delivery of oxygenated blood to tissue. We foresee a role for MSOT diagnosis of vascular diseases of the extremities, which should be studied in patients in the future. In particular, the sensitivity of MSOT to hemoglobin makes it a promising modality for vascular imaging applications.

Disclosures of Conflicts of Interest: A.T. disclosed no relevant relationships. **A.C.T.** disclosed no relevant relationships. **P.C.W.** disclosed no relevant relationships. **M.K.** Activities related to the present article: disclosed no relevant relationships. Activities not related to the present article: is an employee of iThera Medical. Other relationships: has a patent US20140221810 A1 pending, a patent EP2742854A1 pending, and a patent CN103860140A issued. **G.M.v.D.** disclosed no relevant relationships. **V.N.** Activities related to the present article: disclosed no relevant relationships. Activities not related to the present article: is a shareholder of iThera Medical. Other relationships: has US 20140198606 A1 / EP2754388A1, WO 2012103903 A1, WO 2011000389 A1, EP2148183, PCT/EP2008/006142, and US 61/066,187; PCT/EP2009/001137 patents issued and patent WO201109810 1A1, PCT/EP2010/006937 licensed by SurgOptics B.V.

References

1. Wennberg PW. Approach to the patient with peripheral arterial disease. Circulation 2013;128(20):2241–2250.
2. Norgren L, Hiatt WR, Dormandy JA, et al. Inter-Society Consensus for the Management of Peripheral Arterial Disease (TASC II). J Vasc Surg 2007;45(Suppl S):S5–S67.
3. Bradbury AW, Adam DJ, Bell J, et al. Bypass versus Angioplasty in Severe Ischaemia of the Leg (BASIL) trial: analysis of amputation free and overall survival by treatment received. J Vasc Surg 2010;51(5 Suppl):18S–31S.
4. Conte MS. Bypass versus Angioplasty in Severe Ischaemia of the Leg (BASIL) and the (hoped for) dawn of evidence-based treatment for advanced limb ischemia. J Vasc Surg 2010;51(5 Suppl):69S–75S.
5. Owen DR, Lindsay AC, Choudhury RP, Fayad ZA. Imaging of atherosclerosis. Annu Rev Med 2011;62:25–40.
6. Ntziachristos V, Razansky D. Molecular imaging by means of multispectral optoacoustic tomography (MSOT). Chem Rev 2010;110(5):2783–2794.
7. Taruttis A, van Dam GM, Ntziachristos V. Mesoscopic and macroscopic optoacoustic imaging of cancer. Cancer Res 2015;75(8):1548–1559.
8. Zackrisson S, van de Ven SM, Gambhir SS. Light in and sound out: emerging translational strategies for photoacoustic imaging. Cancer Res 2014;74(4):979–1004.
9. Heijblom M, Piras D, Xia W, et al. Visualizing breast cancer using the Twente photoacoustic mammoscope: what do we learn from twelve new patient measurements? Opt Express 2012;20(11):11582–11597.
10. Ermilov SA, Khamapirad T, Conjusteau A, et al. Laser optoacoustic imaging system for detection of breast cancer. J Biomed Opt 2009;14(2):024007.
11. Herzog E, Taruttis A, Beziere N, Lutich AA, Razansky D, Ntziachristos V. Optical imaging of cancer heterogeneity with multispectral optoacoustic tomography. Radiology 2012;263(2):461–468.
12. Laufer J, Johnson P, Zhang E, et al. In vivo preclinical photoacoustic imaging of tumor vasculature development and therapy. J Biomed Opt 2012;17(5):056016.
13. Zhang EZ, Laufer JG, Pedley RB, Beard PC. In vivo high-resolution 3D photoacoustic imaging of superficial vascular anatomy. Phys Med Biol 2009;54(4):1035–1046.
14. Zhang HF, Maslov K, Stoica G, Wang LV. Functional photoacoustic microscopy for high-resolution and noninvasive in vivo imaging. Nat Biotechnol 2006;24(7):848–851.
15. Omar M, Soliman D, Gateau J, Ntziachristos V. Ultrawideband reflection-mode optoacoustic mesoscopy. Opt Lett 2014;39(13):3911–3914.
16. Zhang C, Maslov K, Hu S, et al. Reflection-mode submicron-resolution in vivo photoacoustic microscopy. J Biomed Opt 2012;17(2):020501.
17. Dima A, Ntziachristos V. Non-invasive carotid imaging using optoacoustic tomography. Opt Express 2012;20(22):25044–25057.
18. Niederhauser JJ, Jaeger M, Lemor R, Weber P, Frenz M. Combined ultrasound and optoacoustic system for real-time high-contrast vascular imaging in vivo. IEEE Trans Med Imaging 2005;24(4):436–440.
19. Kolkman RG, Brands PJ, Steenbergen W, van Leeuwen TG. Real-time in vivo photoacoustic and ultrasound imaging. J Biomed Opt 2008;13(5):050510.
20. Fronheiser MP, Ermilov SA, Brecht HP, et al. Real-time optoacoustic monitoring and three-dimensional mapping of a human arm vasculature. J Biomed Opt 2010;15(2):021305.
21. Kim C, Erpelding TN, Jankovic L, Wang LV. Performance benchmarks of an array-based hand-held photoacoustic probe adapted from a clinical ultrasound system for non-invasive sentinel lymph node imaging. Philos Trans A Math Phys Eng Sci 2011;369(1955):4644–4650.
22. Buehler A, Kacprowicz M, Taruttis A, Ntziachristos V. Real-time handheld multispectral optoacoustic imaging. Opt Lett 2013;38(9):1404–1406.
23. Fitzpatrick TB. The validity and practicality of sun-reactive skin types I through VI. Arch Dermatol 1988;124(6):869–871.
24. Rosenthal A, Razansky D, Ntziachristos V. Fast semi-analytical model-based acoustic inversion for quantitative optoacoustic tomography. IEEE Trans Med Imaging 2010;29(6):1275–1285.
25. Dean-Ben XL, Ntziachristos V, Razansky D. Acceleration of optoacoustic model-based reconstruction using angular image discretization. IEEE Trans Med Imaging 2012;31(5):1154–1162.
26. Taruttis A, Rosenthal A, Kacprowicz M, Burton NC, Ntziachristos V. Multiscale multispectral optoacoustic tomography by a stationary wavelet transform prior to unmixing. IEEE Trans Med Imaging 2014;33(5):1194–1202.
27. Jansen K, van der Steen AF, Wu M, et al. Spectroscopic intravascular photoacoustic imaging of lipids in atherosclerosis. J Biomed Opt 2014;19(2):026006.
28. Luke GP, Yeager D, Emelianov SY. Biomedical applications of photoacoustic imaging with exogenous contrast agents. Ann Biomed Eng 2012;40(2):422–437.
29. Taruttis A, Wildgruber M, Kosanke K, et al. Multispectral optoacoustic tomography of myocardial infarction. Photoacoustics 2012;1(1):3–8.
30. Kruger RA, Kuzmiak CM, Lam RB, Reinecke DR, Del Rio SP, Steed D. Dedicated 3D photoacoustic breast imaging. Med Phys 2013;40(11):113301.
31. Cox B, Laufer JG, Arridge SR, Beard PC. Quantitative spectroscopic photoacoustic imaging: a review. J Biomed Opt 2012;17(6):061202.
32. Tzoumas S, Deliolanis N, Morscher S, Ntziachristos V. Unmixing molecular agents from absorbing tissue in multispectral optoacoustic tomography. IEEE Trans Med Imaging 2014;33(1):48–60.